

## Accepted Manuscript

Biological properties and structural study of new aminoalkyl derivatives of benzimidazole and benzotriazole, dual inhibitors of CK2 and PIM1 kinases

K. Chojnacki, P. Wińska, M. Wielechowska, E. Łukowska-Chojnacka, C. Tölzer, K. Niefind, M. Bretner

PII: S0045-2068(18)30274-8  
DOI: <https://doi.org/10.1016/j.bioorg.2018.06.022>  
Reference: YBIOO 2402

To appear in: *Bioorganic Chemistry*

Received Date: 20 March 2018  
Revised Date: 15 June 2018  
Accepted Date: 18 June 2018

Please cite this article as: K. Chojnacki, P. Wińska, M. Wielechowska, E. Łukowska-Chojnacka, C. Tölzer, K. Niefind, M. Bretner, Biological properties and structural study of new aminoalkyl derivatives of benzimidazole and benzotriazole, dual inhibitors of CK2 and PIM1 kinases, *Bioorganic Chemistry* (2018), doi: <https://doi.org/10.1016/j.bioorg.2018.06.022>

This is a PDF file of an unedited manuscript that has been accepted for publication. As a service to our customers we are providing this early version of the manuscript. The manuscript will undergo copyediting, typesetting, and review of the resulting proof before it is published in its final form. Please note that during the production process errors may be discovered which could affect the content, and all legal disclaimers that apply to the journal pertain.



Biological properties and structural study of new aminoalkyl derivatives of benzimidazole and benzotriazole, dual inhibitors of CK2 and PIM1 kinases.

K. Chojnacki<sup>a</sup>, P. Wińska<sup>a</sup>, M. Wielechowska<sup>a</sup>, E. Łukowska-Chojnacka<sup>a</sup>, C. Tölzer<sup>b</sup>, K. Niefind<sup>b</sup>, M. Bretner<sup>a</sup>

<sup>a</sup> Faculty of Chemistry, Warsaw University of Technology, Noakowskiego 3, 00-664 Warsaw, Poland

<sup>b</sup> Department für Chemie, Institut für Biochemie, Universität zu Köln, Zùlpicher Straße 47, D-50674 Köln, Germany

## Abstract

The new aminoalkyl- substituted derivatives of known CK2 inhibitors 4,5,6,7-tetrabromo-1*H*-benzimidazole (TBBi) and 4,5,6,7-tetrabromo-1*H*-benzotriazole (TBBt) were synthesized, and their influence on the activity of recombinant human CK2 $\alpha$ , CK2 holoenzyme and PIM1 kinases was evaluated. All derivatives inhibited the activity of studied kinases and the most efficient were aminopropyl- derivatives **8b** and **14b**. These compounds also exerted inhibition of cancer cell lines - CCRF-CEM (acute lymphoblastoid leukemia), MCF-7 (human breast cancer), and PC-3 (prostate cancer) proliferation and their EC<sub>50</sub> is comparable with the value for clinically studied CK2 inhibitor CX-4945. Preliminary structure activity relationship analysis indicated that the spacer length affected antitumor potency, and two to three methylene units were more favorable. The complex of CK2 $\alpha$ <sup>1-335</sup>/**8b** was crystallized, both under high-salt conditions and under low-salt conditions giving crystals which diffracted X-rays to about 2.4 Å resolution, what enabled the determination of the corresponding 3D-structures.

Keywords: casein kinase 2 CK2; protein kinase PIM1; ATP-competitive inhibitors; antiproliferative activity, structural study

## 1. Introduction

Protein kinases catalyze the transfer of phosphate groups from adenosine triphosphate (ATP) to serine, threonine, or tyrosine residues of target proteins. This phosphorylation is an important stage in regulation of cell growth, cellular signal transduction, cell differentiation, and influences apoptotic mechanisms. Deregulation of protein kinases activity or expression

is implicated in a number of diseases, including cancer, diabetes, and inflammation. Thus, targeted inhibition of the deregulated protein kinases has become an attractive therapeutic strategy in cancer therapy. Casein kinase 2 (CK2) and PIM kinase (Proviral Integration site of Moloney Virus) belong to the serine/threonine kinases family and their overexpression is frequently associated with acute myeloid leukemia, and a variety of cancers including prostate, breast or/and lung cancers [1,2]. The high activity of these kinases in cancer cells is associated with inhibition of apoptosis, suggesting a protective role of CK2 and PIM1 in programmed cell death. Recent studies have shown that the contribution of CK2 and PIM1 kinases in regulation of transcription, differentiation, or signalling of DNA damage/repair systems is achieved by regulating survival pathways. For example, both kinases participate in an activation of the transcriptional factor NF- $\kappa$ B, observed in transformed cells [3, 4]. Elevated level of CK2 induces abnormal activation of NF- $\kappa$ B, which in turn contributes to the development of breast cancer [5]. Moreover, the tumor transformation of lymphocytes with PIM involvement is dependent on activation of NF- $\kappa$ B [4]. Downregulation of these kinases by chemical methods promotes apoptosis in cells [6], indicating CK2 and PIM1 kinases as molecular targets in the development of new therapeutic agents.

Many PIM inhibitors have been reported to date [7, 8, 9,] however, none of them has been marketed so far. SGI-1776 is a representative first-generation PIM inhibitor, which had been under clinical trials for leukemia and prostate cancer [10]. While most of the first-generation PIM inhibitors are PIM1-selective, there is currently great interest in the potential of pan-PIM inhibitors to treat cancer because the three PIM kinases are reported to function redundantly [11]. Representative pan-PIM inhibitors are AZD1208 from AstraZeneca, [12] and PIM447 from Novartis [11]. Clinical trials of PIM447 are underway [11].

Among several classes of CK2 inhibitors effectively inhibiting the growth of tumor cells *in vitro* at low micromolar ranges are derivatives of benzotriazole and benzimidazole e.g. 4,5,6,7-tetrabromo-1*H*-benzotriazole (TBBt), 4,5,6,7-tetrabromo-1*H*-benzimidazole (TBBi), 4,5,6,7-tetrabromo-1*H*-benzimidazole-2-*N,N*-dimethylamine (DMAT), 4,5,6,7-tetraiodo-1*H*-benzimidazole (TIBI), (K<sub>i</sub> 23 nM), and one of the most efficient CK2 and PIM dual inhibitors TDB (K<sub>i</sub> 32 nM, and 86 nM respectively) [13, 14].

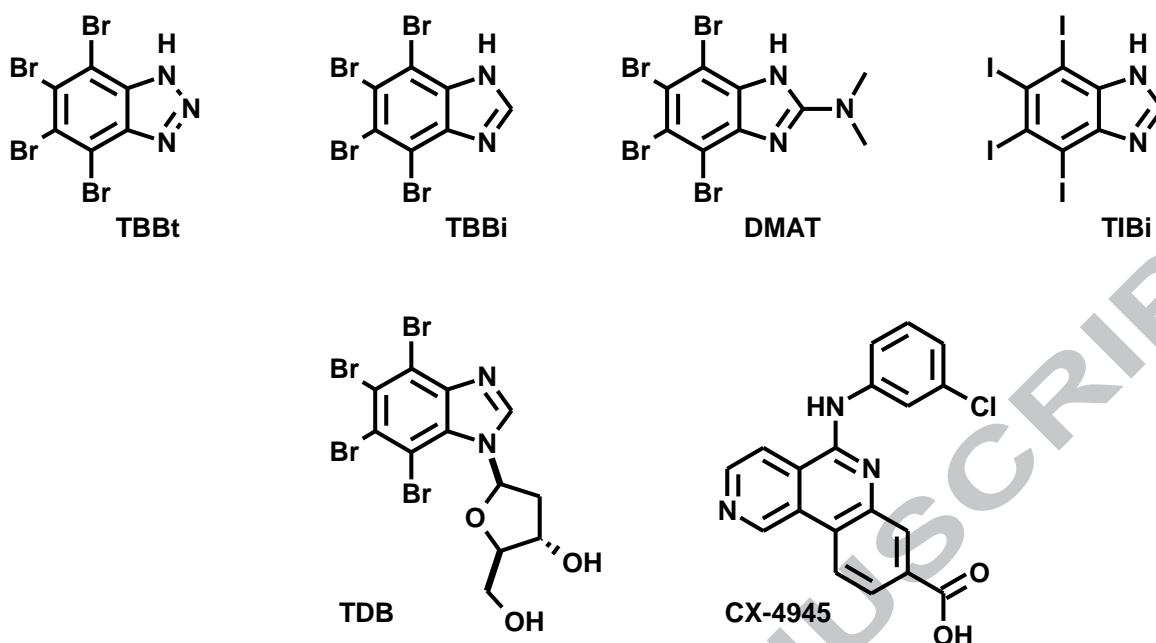


**Figure 1.** The known CK2 inhibitors, derivatives of 1H-benzotriazole, 1H-benzimidazole and CX-4945

Studies conducted by us [15], as well as others [14] show that CK2 inhibitors frequently exhibit similar inhibitory activity against the PIM1 kinase due to structural similarities within the structures of both kinases [16]. CX-4945 (Silmitasertib), the first ATP-competitive CK2 kinase inhibitor that is currently in Phase I/II clinical trials, also inhibits *in vitro* not only CK2 kinase activity, but also PIM1 and PIM2 kinase with IC<sub>50</sub> values of 0.048 and 0.186  $\mu$ M, respectively [7,17]. Recent studies have shown that the use of dual inhibitors (CK2 and PIM inhibition) results in reduced proliferation and induction of apoptosis in human T lymphoblastoid cells (CML) and their multidrug resistant variant (R-CEM), human cervical cancer cells (HeLa) [14] as well as some other cell lines [18].

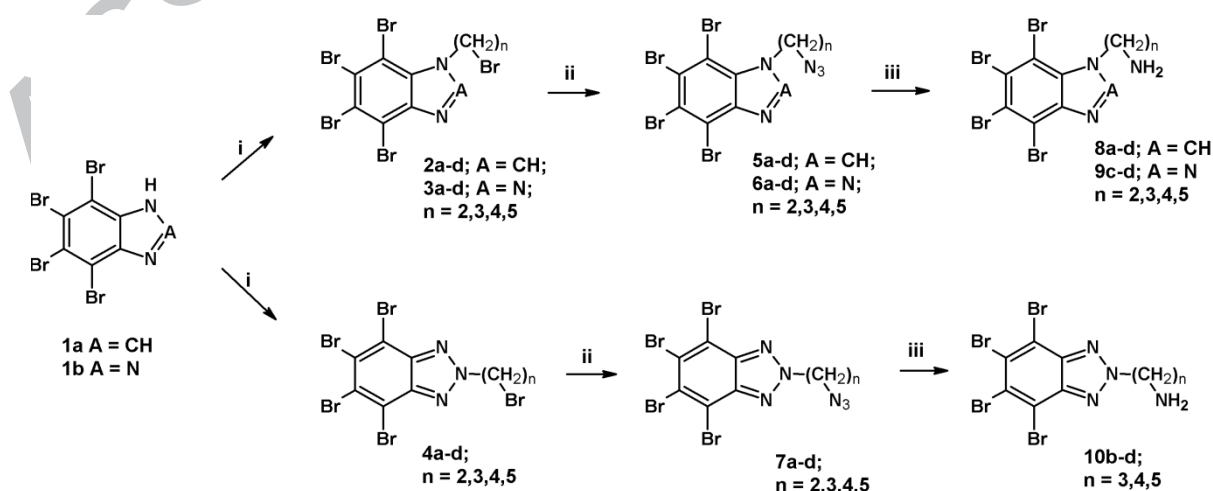
Continuing our search for CK2 inhibitors we synthesized the new azidoalkyl-, and aminoalkyl- substituted derivatives of known inhibitors TBBi and TBBt. The influence of new derivatives on activity of CK2 $\alpha$ , and CK2 holoenzyme was evaluated. We also examined their influence on the kinase PIM1 activity, and on few other kinases to explore the specificity of new compounds. Simultaneous inhibition of the activity of several kinases is a disadvantage when examining the role of different kinases in the cell metabolism or neoplastic transformation, but it can be beneficial in the search for potential anti-cancer drugs.

We previously found that the introduction of a methyl group on the C2 atom of TBBi led to the 4,5,6,7-tetrabromo-2-methyl-1*H*-benzimidazole (2MeTBBi) with a promising inhibitory activity of CK2 and PIM1 and with increased cytotoxicity against CCRF-CEM and MCF-7 cells [19]. Here we report the experimental details of the synthesis of a new series aminoalkyl derivatives of TBBt, TBBi and 2MeTBBi. The inhibitory activity of the synthesized compounds was tested using a standard isoptopic kinase assay and the selectivity of selected compounds against a panel of 8 kinases was determined and compared with selectivity of known inhibitors. The Antiproliferative activity of new compounds was tested against three different cancer cell lines. A crystallographic study of CK2 $\alpha$ -inhibitor complexes was performed in order to investigate the enzyme/inhibitor interactions.

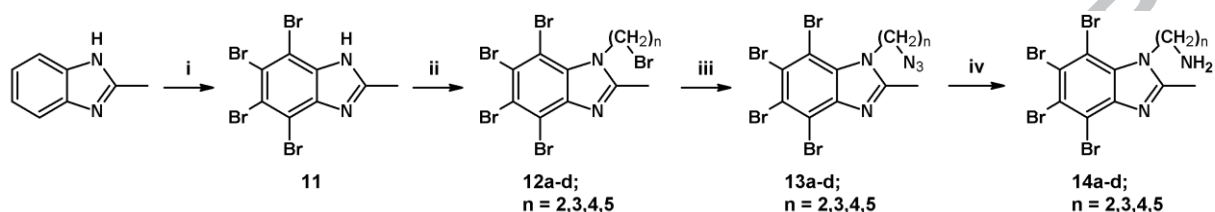
## 2. Results and discussion

### 2.1. Chemistry

The synthesis of the halogenoalkyl derivatives **2a-d**, **3a-d** and **4b-d** was carried out using as starting materials the 4,5,6,7-tetrabromo-1*H*-benzimidazole **1a**, 4,5,6,7-tetrabromo-1*H*-benzotriazole **1b** (Scheme 1), or 4,5,6,7-tetrabromo-2-methyl-1*H*-benzimidazole **11**, (Scheme 2). Alkylation of **1a**, **1b** or **11** with the 1,2-dibromoethane, 1,4-dibromobutane or 1,5-dibromopentane in acetonitrile in the presence of DBU as a base gave **2a,c-d**, **3a,c-d**, **4c-d** and **12a,c-d**, or with the 1-bromo-3-chloropropane gave derivatives **2b**, **3b**, **4b** and **12b**. The azidoalkyl- derivatives with different length of the alkyl chain **5a-d**, **6a-d**, **7a-d** and **13a-d**, were obtained according to known procedures [15] by treatment appropriate halogenoalkyl-derivative with sodium azide in DMF.



**Scheme 1.** Synthetic route to the TBBi and TBBt derivatives: i) dibromoalkyl or chlorobromoalkyl, DBU, CH<sub>3</sub>CN, rt, 72 h; ii) NaN<sub>3</sub>, DMF, 40°C, 24 h; iii) Ph<sub>3</sub>P, THF/H<sub>2</sub>O, rt, 48 h.



**Scheme 2.** Synthetic route to the 4,5,6,7-tetrabromo-2-methyl-1H-benzimidazole derivatives: i) Br<sub>2</sub>, H<sub>2</sub>O, reflux, 72 h; ii) dibromoalkyl, DBU, CH<sub>3</sub>CN, rt, 2-9 days; iii) NaN<sub>3</sub>, DMF, 60°C, 24 h; iv) Ph<sub>3</sub>P, THF/H<sub>2</sub>O, rt, 48 h.

The reduction of alkylazido derivatives was performed with the use of Ph<sub>3</sub>P in THF/H<sub>2</sub>O. After completion of the reaction products were purified by column chromatography to obtain TBBi aminoalkyl- derivatives **8a-d** in good yields (70-86%), TBBt aminoalkyl- derivatives **9c-d** and **10b-d** in yields ranging from 44% to 93% and 2MeTBBi aminoalkyl- derivatives **14a-d** in yields ranging from 64% to 96%. The synthesis of compounds **9a-b** and **10a** was unsuccessful with the use of this method. The structures of the new compounds were confirmed by analytical data, including high resolution mass spectra (MS or FTMS), <sup>1</sup>H and <sup>13</sup>C NMR.

## 2.2. Evaluation of biological activity

### 2.2.1. Kinases inhibition study

The influence of azidoalkyl- derivatives **5a-d**, **6a-d**, **7a-d**, and aminoalkyl- derivatives **8a-d**, **9c-d**, **10b-d**, **14a-d** on the human CK2 $\alpha$ , and PIM1 activity was evaluated using radiometric assay, and the results are shown in Table 1. The synthetic peptide RRRADDSDDDD was used as the substrate of CK2 and peptide ARKRRRHPSGPPTA as the substrate of PIM1. Screening studies of inhibitory activity of obtained derivatives were performed in the presence of 5  $\mu$ M and 10  $\mu$ M compounds and subsequently, the percent of residual activity of CK2 $\alpha$  and PIM1 was calculated. K<sub>i</sub> values were determined for the most active compounds for both human CK2 $\alpha$  and CK2 holoenzyme, as well as for PIM1.

Among derivatives with azidoalkyl- substituents the CK2 $\alpha$  activity was inhibited most effectively by the TBBi derivative **5a** with the azido group linked by a two-carbon alkyl chain to benzimidazole scaffold, but it was less effective than parent TBBi ( $K_i$  2.3  $\mu$ M *versus* 0.58  $\mu$ M). Furthermore, the activity of the PIM1 kinase was inhibited with the same efficiency by compound **5a** and TBBi. On the other hand azidoalkyl- TBBt derivatives **6a-d** and **7a-d** showed a very weak inhibition of both CK2 and PIM kinase activity.

The reduction of azido groups to amine led to the new derivatives with aminoalkyl- substituents, which appeared to be more effective inhibitors of both kinases. Among the synthesized new aminoalkyl-TBBi derivatives, we found three potent inhibitors of CK2 which inhibited more than 50% activity of enzyme at a concentration of 5  $\mu$ M (**8b,c,d**), with  $K_i$  for CK2 $\alpha$  in the range 0.75-1.35  $\mu$ M and  $K_i$  for holoenzyme CK2 in the range of 0.17-0.23  $\mu$ M, comparable to  $K_i$  0.15  $\mu$ M for TBBi. These TBBi derivatives appeared to be also potent inhibitors of kinase PIM1, with an inhibition more than 90% activity at a concentration of 5  $\mu$ M and  $K_i$  for PIM1 in the range 0.19-0.27  $\mu$ M also comparable to  $K_i$  for TBBi 0.27  $\mu$ M.

Moreover, replacement of TBBi by TBBt led to less potent inhibitors. *N*1-TBBt derivatives **9c-d** at 5 $\mu$ M concentration inhibited 40-50% activity of both enzymes, while *N*2-TBBt derivatives **10b-d** were found to inhibit more effectively PIM1 activity than CK2 $\alpha$  activity.

**Table 1.** The residual activity (%) of CK2 $\alpha$ , holoenzyme CK2 and PIM1 in the presence of alkylazido-TBBi (**5a-d**) alkylazido-TBBt (**6a-d**, **7a-d**), aminoalkyl-TBBi (**8a-d**), aminoalkyl-TBBt derivatives (**9c,d**; **10b-d**) and alkylamino-2-MeTBBi (**14a-d**) derivatives.

Compd.	Residual activity of CK2 $\alpha$ [%] or $K_i^*$ [ $\mu$ M]			CK2 holoenzyme	Residual activity of PIM1 [%] or $K_i^*$ [ $\mu$ M]		
	5 $\mu$ M	10 $\mu$ M	$K_i^*$ [ $\mu$ M]	$K_i^*$ [ $\mu$ M]	5 $\mu$ M	10 $\mu$ M	$K_i^*$ [ $\mu$ M]
<b>5a</b>	48.6	36.6	2.30	-	12.5	10.5	-
<b>5b</b>	54.3	44.4	3.15	-	22	9.3	-
<b>5c</b>	62.2	34	-	-	31.7	15.4	-
<b>5d</b>	62	50	-	-	45	33.2	-
<b>6a</b>	87	73	-	-	78.5	73.5	-
<b>6b</b>	95	90	-	-	97	81	-
<b>6c</b>	99	86	-	-	89	87	-
<b>6d</b>	100	98	-	-	99.7	94	-
<b>7a</b>	96	95	-	-	85	83.5	-

<b>7b</b>	81	79	-	-	94	93	-
<b>7c</b>	88	87	-	-	89	87	-
<b>7d</b>	100	100	-	-	97.8	90	-
<b>8a</b>	75	50	-	0.77	10.2	5.8	0.48
<b>8b</b>	34	20	1.20	0.17	9.6	4.5	0.19
<b>8c</b>	24	12	0.77	0.19	9.5	4.7	0.27
<b>8d</b>	36	23	1.35	0.23	8.1	4.6	0.22
<b>9c</b>	58	43	-	0.71	54	34	-
<b>9d</b>	60	46	-	-	47	25	-
<b>10b</b>	67	49	-	0.55	24.7	14	0.80
<b>10c</b>	85	62	-	1.2	34	21	1.10
<b>10d</b>	64	50	-	-	28	14	-
<b>14a</b>	34	19.5	1.81	0.44	2.7	1.5	0.09
<b>14b</b>	23	13	0.82	0.18	2.1	1.5	0.08
<b>14c</b>	17	8.6	0.78	0.22	3.2	1.3	0.10
<b>14d</b>	30	19	1.01	0.44	1.2	0.6	0.05
<b>11</b>	-	-	1.07	-	6 <sup>[19]</sup>	-	-
<b>TBBi</b>	20	12	0.58	0.15	14	7.6	0.27
<b>TBBt</b>	4.6	2.2	0.17	0.04	19.6	9	0.50

\*K<sub>i</sub> values were calculated using Cheng and Prusoff equation:  $K_i = IC_{50}/(1 + [S]/K_m)$  [20]

The introduction of additional methyl group to C2 carbon in TBBi had little effect on inhibitory properties towards CK2 $\alpha$  kinase (K<sub>i</sub> in the range 0.78-1.81  $\mu$ M) and holoCK2 (K<sub>i</sub> 0.18-0.44  $\mu$ M for **14a-d** vs 0.17-0.77  $\mu$ M for **8a-d**) but significantly affected PIM1 inhibition (K<sub>i</sub> 0.05-0.10  $\mu$ M for **14a-d** vs 0.19-0.48  $\mu$ M for **8a-d**). Among the aminoalkyl- derivatives **14a-d** the most potent inhibitors of both CK2 and PIM1 kinases were compounds **14b** and **14c**, which displayed similar K<sub>i</sub> as TBBi for CK2 $\alpha$  and holoCK2, and lower K<sub>i</sub> than compound **11**, and much lower K<sub>i</sub> for PIM1 (0.08 – 0.10  $\mu$ M vs 0.27  $\mu$ M for TBBi).

### 2.2.2. Kinase profile

The effect of some new derivatives on the activity of other kinases, especially those, which activity is usually inhibited by the TBBi, TBBt and their derivatives, was also examined. Specificity studies were performed in ProKinase GmbH, Freiburg, Germany (**8b**,

**14b**), and data for compounds TBBi, TBBt and CX-4945 are taken from a previous publications [21, 22].

Table 2. *In vitro* residual enzymatic activity (%) of 9 kinases in the presence of **8b** and **14b** derivatives (selectivity profile)

Kinase group	Other	CK1	CAMK	CMGC	CMGC	CMGC	CMGC	CAMK	AGC	CAMK
Kinase	CK2 $\alpha$	CK1- $\alpha$ 1	PIM1	CDK2	DYRK1A	CLK2	HIPK2	IKK $\alpha$	PKA	PKD2
Compound	Residual activity (%) in the presence of 5 $\mu$ M compounds (or 10 $\mu$ M, comp. <b>TBBi</b> and <b>TBBt</b> ) <sup>[21]</sup> and (0.5 $\mu$ M CX-4945) <sup>[22]</sup>									
<b>TBBi</b> <sup>[21]</sup>	20	48	14	23	3	-	3	37[IKK $\beta$ ]	75	5[PKD1]
2Me <b>TBBi</b> <sup>[19]</sup>	K <sub>i</sub> 1.11	84	6	20	17	-	43	-	113	14
<b>8b</b>	34	42	9.6	22	31	15	34	28	70	39
<b>14b</b>	23	63	2.1	21	47	10	30	29	84	35
<b>TBBt</b> <sup>[21]</sup>	4.6	61	19.6	48	4	-	5	58[IKK $\beta$ ]	45	37[PKD1]
CX-4945 <sup>[22]</sup>	0	95[CK1 $\beta$ ]	6	40	5[DYRK2]	0[CLK3]	15	102	78	-

As shown at Table 2, compounds **8b** and **14b** exhibited similar inhibitory activity to the studied kinases as other TBBi or TBBt derivatives reported previously [21], **8b** inhibits more efficiently PIM1 (Table 1) CDK2, CLK2 and less efficiently CK1 and PKA kinases than CK2 $\alpha$ , **14b** inhibits more successfully PIM1 (Table 1), CLK2 and less CK1, DYRK1A and PKA kinases than CK2 $\alpha$ , but the differences in the rate of inhibition are not big; and CX-4945 at 0.5  $\mu$ M inhibits the activity of DYRK2, CLK3 and PIM1 (6%, [22]).

### 2.2.3. Antiproliferative activity

To determine how inhibition of CK2 and PIM1 kinases affects the viability of different cancer cell lines: CCRF-CEM (leukemia), MCF-7 (breast) and PC-3 (prostate), we selected the most active inhibitors **8a-d**, **10b** and **14a-d** for *in vitro* studies and compared their influence with the known potent and selective inhibitor of CK2, CX-4945. The cells were treated with different concentration of compounds for 48 h.

The EC<sub>50</sub> values were determined to express the concentration of compound which lowered the viability of the cells to 50% in comparison to cells cultures not treated with inhibitors and the results are collected in Table 3.

Table 3. The influence of new aminoalkyl- derivatives **8a-d** and **14a-d** on the viability of CCRF-CEM, MCF-7 and PC-3 cell lines

compound	CCRF-CEM EC <sub>50</sub> [ $\mu$ M]	MCF-7 EC <sub>50</sub> [ $\mu$ M]	PC-3 EC <sub>50</sub> [ $\mu$ M]	clogP <sup>a</sup>	solub <sup>a</sup> mg/mL
<b>8a</b>	4.3 $\pm$ 0.8	6.0 $\pm$ 0.1	8.2 $\pm$ 0.4	3.76	0.47
<b>8b</b>	6.3 $\pm$ 0.1	8.8 $\pm$ 0.3	12.1 $\pm$ 1.1	3.82	1.69
<b>8c</b>	8.0 $\pm$ 0.9	12.7 $\pm$ 0.4	16.1 $\pm$ 2.1	4.34	1.41
<b>8d</b>	6.7 $\pm$ 0.1	8.2 $\pm$ 0.4	10.2 $\pm$ 0.9	4.78	0.87
<b>10b</b>	9.0 $\pm$ 0.3	9.6 $\pm$ 0.4	16.7 $\pm$ 2.3	3.82	7.33
<b>14a</b>	0.7 $\pm$ 0.02	0.9 $\pm$ 0.03	1.4 $\pm$ 0.4	3.8	1.35
<b>14b</b>	2.1 $\pm$ 0.3	3.4 $\pm$ 0.2	4.4 $\pm$ 0.4	3.94	4.89
<b>14c</b>	7.5 $\pm$ 1.7	10 $\pm$ 0.4	14.2 $\pm$ 0.8	4.46	4.13
<b>14d</b>	4.8 $\pm$ 0.5	6.8 $\pm$ 0.1	8.9 $\pm$ 0.8	4.91	2.56
<b>TBBI</b>	14.2 $\pm$ 2.8	15.7 $\pm$ 0.5	17.5 $\pm$ 0.1	4.33	<0.01
<b>TBBt</b>	>50	>50	>50	4.38	<0.01
<b>2MeTBBI</b>	<10	> 20	n.d.	4.46	<0.01
<b>CX-4945</b>	3.1 $\pm$ 0.50	8.4 $\pm$ 0.35	10.4 $\pm$ 0.1	3.29	0.37

The reported values represent the means  $\pm$  SD from three parallel experiments.

<sup>a</sup>Calculator plugins were used for clogP and solubility at pH 7.4 ChemAxon <http://chemicalize.com>

All new derivatives reduced the viability of studied cancer cell lines at lower concentrations than their parent compounds TBBI, TBBt and 2MeTBBI. The most sensitive was the CCRF-CM cell line with EC<sub>50</sub> values for compounds **8a-d** in the range of 4-8  $\mu$ M, and for derivatives **14a-d** in the range of 0.7-7.5  $\mu$ M, while for CX-4945 EC<sub>50</sub> was 3.1  $\mu$ M. (Table 3). TBBt derivative (compound **10b**) presented rather a moderate cytotoxic activity against studied cell lines (EC<sub>50</sub> values in the range 9-16.7  $\mu$ M) but still much higher than TBBI (EC<sub>50</sub> > 50  $\mu$ M) or TBBi (EC<sub>50</sub> 14.2-17.5  $\mu$ M). More efficient in inhibiting of cell viability were derivatives of 2MeTBBI (**14a-d**) than TBBI derivatives (**8a-d**) also in relation to the viability of other tested cell lines.

The determined EC<sub>50</sub> value for the most potent compounds were as follow: for **14a** 0.7 $\pm$ 0.02  $\mu$ M; 0.9 $\pm$ 0.03  $\mu$ M; 1.4 $\pm$ 0.4  $\mu$ M and for **14b** 2.1 $\pm$ 0.3  $\mu$ M; 3.4 $\pm$ 0.2  $\mu$ M; 4.4 $\pm$ 0.4  $\mu$ M, while for CX-4945 were 3.1 $\pm$ 0.50  $\mu$ M; 8.4 $\pm$ 0.35  $\mu$ M; 10.4 $\pm$ 0.1  $\mu$ M for CCRF-CEM, MCF-7

and PC-3 cells, respectively. The higher activity of new derivatives having a methyl group on carbon 2 in the imidazole ring (compounds **14a-d**) may be associated with higher solubility of these derivatives in aqueous solutions (see Table 3).

We also examined the influence of the spacer length of aminoalkyl derivatives on cytotoxic activities. The data collected in Table 3 showed that compounds **8c,d** and **14c,d** with a spacer of four to five methylene units exhibited lower cytotoxic activities, than compounds **8a,b** and **14a,b** with the spacer of two or three methylene units.

### 2.3. Structural study

In order to clarify the binding mode of **8b** (Figure 2) to the active site of CK2 $\alpha$  we co-crystallized CK2 $\alpha^{1-335}$ , a C-terminally truncated version of human CK2 $\alpha$  [23], with the inhibitor. Previous comparative structure analyses with different CK2 inhibitors [24, 25] had shown that the local enzyme conformation next to the ligand or the orientation and conformation of the ligand or both can vary to a certain degree on the salt content of the crystallization medium and that in particular halogen bonds with aromatic rings can be strongly salt-dependent [24, 25]. Therefore, we crystallized the CK2 $\alpha^{1-335}$ /**8b** complex, both under high-salt conditions (with NaCl as precipitant; structure no. 1 in Table 4) and under low-salt conditions (with PEG3350 as a precipitating agent; structure no. 2 in Table 4). Both types of crystals diffracted X-rays to about 2.4Å resolution and enabled the determination of the corresponding 3D-structures (Figure 2A).

Table 4. Crystallization, X-ray diffraction data and refinement statistics

Structure No.	1	2
PDB code	5OWH	5OWL
<i>Crystallization</i>		
Method	sitting drop variant of vapour diffusion	
Temperature	20 °C	
Reservoir composition	4.4M NaCl, 0.1M citric acid, pH 5.5	25% (w/v) PEG3350, 0.2M ammonium sulfate, 0.1M BIS-TRIS, pH 6.5
Sitting drop composition before equilibration	1µL reservoir + 1µL enzyme/inhibitor mixture (48µL 7.5 mg/mL enzyme, 0.5M NaCl, 25mM Tris/HCl, pH 8.5, mixed and pre-equilibrated with 2 µL 20 mM inhibitor in DMSO)	
<i>X-ray Diffraction Data Collection</i>		
Wavelength [Å]	1.0000	0.9660
Temperature [K]	100	
Synchrotron (beamline)	ESRF (ID23-1)	ESRF (ID23-1)

Space group		P4 <sub>3</sub> 2 <sub>1</sub> 2	P4 <sub>3</sub> 2 <sub>1</sub> 2
Unit cell	a, b, c [Å]	71.66, 71.66, 133.11	126.31, 126.31, 125.21
	$\alpha, \beta, \gamma$ [°]	90.0, 90.0, 90.0	90.0, 90.0, 90.0
Protomers per asymmetric unit		1	2
Resolution [Å] (highest res. shell)		63.100 – 2.376 (2.461 – 2.376) <sup>1</sup>	72.710 – 2.391 (2.477 – 2.391) <sup>1</sup>
R <sub>sym</sub> [%]		9.9 (143.0) <sup>1</sup>	7.2 (106.7) <sup>1</sup>
CC1/2		0.998 (0.536) <sup>1</sup>	0.999 (0.665) <sup>1</sup>
Signal-to-noise ratio (I/ $\sigma$ )		11.92 (1.07) <sup>1</sup>	14.56 (1.51) <sup>1</sup>
No. of unique reflections		14462 (1391) <sup>1</sup>	40314 (3831) <sup>1</sup>
Completeness [%]		98.72 (96.60) <sup>1</sup>	99.16 (95.67) <sup>1</sup>
Multiplicity		7.2 (7.1) <sup>1</sup>	5.0 (4.9) <sup>1</sup>
Wilson B-factor [Å <sup>2</sup> ]		55.07	54.14
<i>Structure Refinement</i>			
No. of reflections for R <sub>work</sub> /R <sub>free</sub>		13436/1026	39250/1037
R <sub>work</sub> /R <sub>free</sub> [%]		21.45/25.96	19.94/23.50
Number of non-H-atoms		2886	5795
	Protein	2817	5608
	Ligand/ion	18	65
	Water	51	122
Aver. B-factor [Å <sup>2</sup> ]		67.25	62.70
	Protein	67.32	62.26
	Ligand/ion	105.78	114.58
	water	49.87	55.10
RMS deviations			
	Bond lengths [Å]	0.003	0.003
	Bond angles [°]	0.53	0.54
Ramachandran plot			
	favoured (%)	96.08	96.18
	allowed (%)	3.92	3.19
	outliers (%)	0.00	0.00

<sup>1</sup>The data in brackets refer to the highest resolution shell.

The low-salt structure contains two independent protein chains per asymmetric unit, the high-salt structure only one. In each of the three protomers an **8b** inhibitor molecule is bound to the ATP site at the interface of the two major domains of the enzyme (Figure 2A). This is consistent to the fact that the ATP site of CK2 $\alpha$  – compared to many other eukaryotic protein kinases – is particularly narrow and hydrophobic [26] and thus prone to accommodate flat and non-polar molecular scaffolds [27].

In the high-salt structure this hydrophobicity driven affinity is supported by five polar interactions of peripheral substituents of **8b** (Figure 2 B) with the protein: three bromine atoms form halogen bonds, namely Br(C7) with the side chain oxygen of Asn118, Br(C6) with the peptide carbonyl oxygen of Val116 and Br(C4) with the aromatic side chain of Phe113; in addition the positively charged amino propyl group forms an ionic contact to the side chain of Asp120 and is hydrogen-bonded to the carbonyl-oxo group of His160 (Figure 1B). Two of these interactions – those with the side chains of Asn118 and Asp120 – are only possible if these side chains are closely enough to the centre of the ATP site, meaning they require a particular local conformation of the enzyme’s interdomain hinge/helix  $\alpha$ D region referred to as “closed” [28] or “Phe121-in” conformation [29] in the literature. Crystallization conditions dominated by precipitating kosmotropic salts support this closed conformation irrespective of the ATP-site ligand [30] because this optimizes the hydrophobic packing within the protein [31]. Insofar, the high sodium chloride concentration in the crystallization medium used to obtain structure 1 indirectly – namely by stabilizing the closed conformation of the hinge/helix  $\alpha$ D region – favours the binding of **8b** with an orientation in which the amino propyl moiety points outwards (Figure 2A/B).

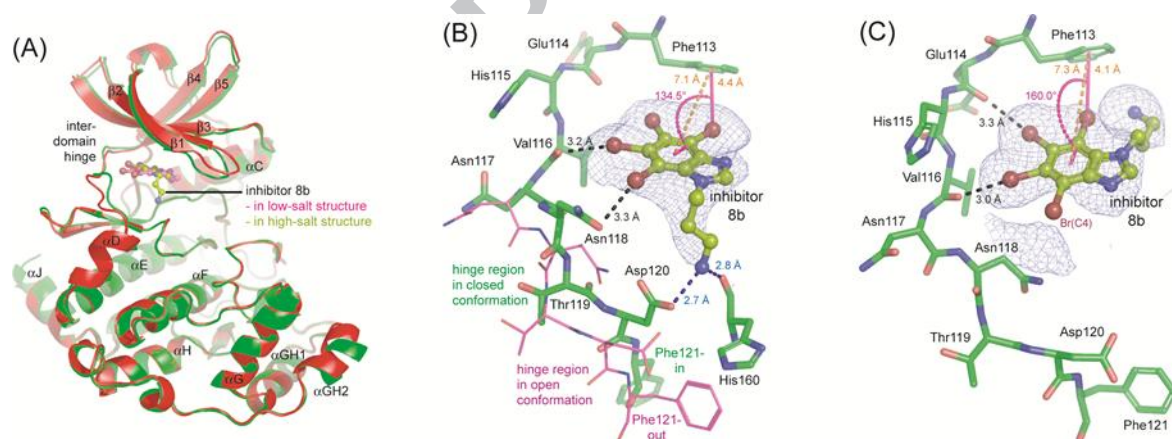


Figure 2: Binding of inhibitor **8b** to CK2 $\alpha$

A) Overview of the high-salt (green) and the low-salt (red) complex structures after 3D-fit. The bound inhibitor is drawn with yellow-green C-atoms in its high-salt orientation and with magenta-coloured C-atoms in its low-salt orientation. B/C) ATP-site with bound inhibitor **8b** in the high-salt structure with a section of the hinge region in the low-structure drawn for comparison with magenta-coloured C-atoms (B) and in the low-salt structure (C) covered with the respective polder OMIT map [32] at a contouring level of 3  $\sigma$ . Halogen bonds are indicated either with black dotted lines (carbonyl oxygen atoms as Lewis bases) or with

orange-coloured dotted lines (phenyl ring  $\pi$ -system as Lewis base) and hydrogen bonds with blue dotted lines. In the case of the  $\pi$ -halogen bonds three typical parameters are given: the distance  $d$  (between the bromine atom and the aromatic ring centroid) and the angle  $\theta$  (between the bromine-carbon bond and the aromatic ring centroid) as defined by Lu et al. [33] and the  $d_2$ -distance between the two aromatic ring centres defined by Matter et al. [34].

Against this background it is not surprising that the binding mode of **8b** under low-salt crystallization conditions (Figure 2 C) in which the hinge region adopts an open conformation (Figure 2 C and also visible for comparison as hinge region section with magenta-coloured C-atoms in Figure 2 B) is different from that of the high-salt state (Figure 2 B). The side chain contacts to Asn118 and Asp120 are no longer possible; consequently, the inhibitor is turned by about 180 degrees around a pseudo-twofold axis running lengthwise through the C2 atom and the two-ring system. Due to this rotation the amino propyl substituent no longer points outwards to the hinge, but inwards to the Ph113 side chain. Three halogen bonds are still present, but now two backbone carbonyl groups are involved (Glu114 and Val116; Figure 2 C). Further, the parameters  $d$ ,  $d_2$  and  $\theta$  fit better to the typical values of  $\pi$ -Br interactions than in the high-salt case where in particular the  $d$  distance is with 4.4Å (Figure 2 B) rather large.

Noteworthy, under low-salt conditions the Br(C4) atom of the inhibitor is covered neither by the polder OMIT map (Figure 2 C) nor by the normal electron density (not shown). Rather there is a significant piece of density next to this atom which is not suitable for filling with a water molecule or another small molecule. Most probably, this is a radiation damage artefact occurring during X-ray diffraction data collection and leading to a break of the covalent bond between the carbon atom C4 and the bromine atom Br(C4) which is not protected in this structure by a halogen bond. A similar phenomenon was observed in a complex structure between the paralogous subunit CK2 $\alpha'$  and a tetrabromo benzotriazole derivative [35] (PDB code 3OFM) in which the enzyme/inhibitor arrangement is quite similar to the low-salt state found here (Figure 2 C).

### 3. Conclusions

In summary, a series of new aminoalkyl- TBBi and TBBt derivatives were synthesized by reduction of the corresponding azidoalkyl- derivatives with quite reasonable yields. The novel aminoalkyl- TBBi derivatives **8b-c** inhibit the activity of CK2 holoenzyme and the PIM1 as effectively as TBBi, while the derivatives of 2MeTBBi (**11**), compounds **14a-b** exerted superior inhibition of PIM1 kinase. The aminoalkyl-TBBt derivatives **9c-d** and **10b-d**

appeared to be weaker inhibitors of CK2 but a little stronger inhibitors of PIM1 than parent TBBt. Evaluation of anti-proliferative activities against CCRF-CEM, MCF-7 and PC-3 human cancer cell lines provided however very interesting results. New alkylamine-derivatives of TBBi and TBBt reduce the viability of cancer cells much more strongly than their parent compounds. Particularly interesting properties have shown derivatives of 2MeTBBi (**11**), compounds **14a-b**, which inhibit the viability of tumor cells even more effectively than the known and approved for clinical trials compound CX-4945. These studies provide evidence for the effectiveness of developing therapies based on the mechanism of a combination of CK2 and PIM kinase inhibitors in the treatment of cancer.

## 4. Experimental

### 4.1. Chemistry

#### 4.1.1 General

Commercially obtained reagents were used as received without additional purification. Melting points were determined with an MPA100 Optimelt SRS apparatus and are uncorrected. NMR spectra were recorded with tetramethylsilane as an internal standard using a Varian NMR System 500 MHz or Varian Mercury 400 MHz or Bruker 500 MHz spectrometers. Chemical shifts are reported in ppm from internal tetramethylsilane standard, splitting patterns have been designated as follows: s = singlet; bs = broad singlet; d = doublet; t = triplet; q = quartet; dd = double doublet; m = multiplet, quin = quintet. Thin layer chromatography (TLC) was carried out on aluminium plates with silica gel Kieselgel 60 F254 (Merck) (0.2 mm thickness film) and detection of compounds was performed after UV light at 254nm. Silica gel with grain size 40-63 $\mu$ m was used for column chromatography. Mass spectrometry were recorded on Micro-mass ESI Q-TOF Premier Waters Spectrometer, and FTMS were recorded on Q Exactive Hybrid Quadrupole-Orbitrap Mass Spectrometer, ESI (electrospray) with spray voltage 4.00 kV. The most intensive signal are reported.

The following compounds were prepared according to previously described by us procedures: 4,5,6,7-tetrabromo-1-(2-bromoethyl)-1*H*-benzimidazole (**2a**) [15], 4,5,6,7-tetrabromo-1-(3-chloropropyl)-1*H*-benzimidazole (**2b**) [36], 4,5,6,7-tetrabromo-1-(2-bromoethyl)-1*H*-benzotriazole (**3a**) [36], 4,5,6,7-tetrabromo-1-(2-bromoethyl)-2*H*-benzotriazole (**4a**) [36], 4,5,6,7-tetrabromo-1-(3-chloropropyl)-1*H*-benzotriazole (**3b**) and 4,5,6,7-tetrabromo-1-(3-chloropropyl)-2*H*-benzotriazole (**4b**) [36], 1-(2-azidoethyl)-4,5,6,7-tetrabromo-1*H*-benzimidazole (**5a**) [36], 1-(3-azidopropyl)-4,5,6,7-tetrabromo-1*H*-

benzimidazole (**5b**) [36], 1-(2-azidoethyl)-4,5,6,7-tetrabromo-1*H*-benzotriazole (**6a**) [36], 1-(3-azidopropyl)-4,5,6,7-tetrabromo-1*H*-benzotriazole (**6b**) [36], 2-(2-azidoethyl)-4,5,6,7-tetrabromo-2*H*-benzotriazole (**7a**) [36], 2-(3-azidopropyl)-4,5,6,7-tetrabromo-2*H*-benzotriazole (**7b**) [36], and the properties are in agreement with published previously.

#### 4.1.2. Synthesis of 4,5,6,7-tetrabromo-2-methyl-1*H*-benzimidazole (**11**).

To the suspension of 2-methyl-1*H*-benzimidazole (1.32 g, 10.0 mmol) in water (80 mL), bromine (10 mL 195 mmol, 19.5 eq.) was added and refluxed over 72 h. After cooling, the precipitate was filtered and washed with water. Crude product was purified by crystallization from methanol. Yield: 4.32 g (96%); Mp. 330°C; MS [M+H]<sup>+</sup> *m/z* calcd for C<sub>8</sub>H<sub>5</sub>Br<sub>4</sub>N<sub>2</sub><sup>+</sup> 448.7812; found 448.6709. <sup>1</sup>H NMR (500 MHz, DMSO-*d*<sub>6</sub>) δ ppm: 2.55 (s, 3H, CH<sub>3</sub>).

#### 4.1.3. General method for the synthesis of aminoalkyl derivatives (**8a-d**; **9c-d**; **10b-d**; **14a-d**):

A three-step reaction sequence was utilized to prepare title products.

A solution of **1a**, **1b** or **11** (2.3 mmol) in acetonitrile (20 mL) was stirred with DBU (5.7 mmol) and 1-2-dibromoethane, 1-bromo-3-chloropropane, 1,4-dibromobutane or 1,5-dibromopentane (16 mmol) at room temperature. After completion of the reaction the reaction mixture was concentrated under reduced pressure. The residue was diluted with water (25 mL) and extracted with chloroform (3 x 25 mL). The combined organic layers were washed with water (50 mL), dried over anhydrous MgSO<sub>4</sub>, filtered, and the solvent was removed under reduced pressure. The residue was purified as specified in each case.

A solution of appropriate halogenoalkyl derivative **2a-d**, **3a-d**, **4a-d**, **12a-d** (1.0 mmol) and NaN<sub>3</sub> (1.3 mmol) in DMF (10 mL) was stirred at 40°C for 24 h. After completion of the reaction (TLC) the reaction mixture was diluted with ethyl acetate (30 mL), washed with water (3 x 30 mL), dried over anhydrous MgSO<sub>4</sub>, filtered, and the solvent was removed under reduced pressure. Products were purified by crystallization or column chromatography.

A solution of appropriate azide **5a-d**, **6a-d**, **7a-d**, **13a-d** (0.56 mmol) and Ph<sub>3</sub>P (0.62 mmol) in THF (6 mL) and H<sub>2</sub>O (0.6 mL) was stirred for 48 h at room temperature. After completion of the reaction (TLC) the reaction mixture was evaporated under reduced pressure. The residue was suspended in sat. NaHCO<sub>3</sub>aq. (25 mL) and extracted with chloroform (3 x 25 mL). The organic layer was dried over anhydrous MgSO<sub>4</sub>, filtered, and the solvent was removed under reduced pressure. Products were purified by column chromatography.

#### 4.1.3.1. 2-(4,5,6,7-Tetrabromo-1H-benzimidazol-1-yl)ethanamine (**8a**).

From **5a**; the product was purified by column chromatography (DCM/MeOH/TEA, 15/1/0.1) to afford **8a** as white solid (72%), Mp.  $T > 253^{\circ}\text{C}$  decomp.; FTMS  $[\text{M}+\text{H}]^{+}$   $m/z$  calcd. for  $\text{C}_9\text{H}_8\text{Br}_4\text{N}_3^{+}$  477.7405, found 477.7403;  $^1\text{H}$  NMR (500 MHz,  $\text{DMSO}-d_6$ )  $\delta$  ppm: 3.14 (t, 2H,  $J = 5.9$  Hz), 4.62 (t, 2H,  $J = 5.9$  Hz), 8.46 (s, 1H);  $^{13}\text{C}$  NMR (125 MHz,  $\text{DMSO}-d_6$ )  $\delta$  ppm: 41.65, 46.91, 106.95, 116.96, 120.79, 122.68, 131.96, 144.20, 149.59.

#### 4.1.3.2. 3-(4,5,6,7-Tetrabromo-1H-benzimidazol-1-yl)propan-1-amine (**8b**).

From **5b**; the product was purified by column chromatography (DCM/MeOH/TEA, 9/1/0.5) to afford **8b** as white solid (70%), Mp.  $132\text{--}134^{\circ}\text{C}$ ; FTMS  $[\text{M}+\text{H}]^{+}$   $m/z$  calcd. for  $\text{C}_{10}\text{H}_{10}\text{Br}_4\text{N}_3^{+}$  491.7562, found 491.7559;  $^1\text{H}$  NMR (500 MHz,  $\text{DMSO}-d_6$ )  $\delta$  ppm: 1.58 (quin, 2H,  $J = 6.9$  Hz), 2.50 – 2.53 (m, 2H), 4.53 (t, 2H,  $J = 6.9$ ), 8.48 (s, 1H);  $^{13}\text{C}$  NMR (125 MHz,  $\text{DMSO}-d_6$ )  $\delta$  ppm: 35.32, 38.58, 44.82, 107.07, 116.97, 120.81, 122.77, 131.78, 144.15, 149.41.

#### 4.1.3.3. 4-(4,5,6,7-Tetrabromo-1H-benzimidazol-1-yl)butan-1-amine (**8c**).

From **1a**, after work-up and purification by column chromatography (DCM) **2c** was obtained as a white solid; Yield 77%; Mp.  $148\text{--}149^{\circ}\text{C}$ ; MS  $[\text{M}+\text{H}]^{+}$   $m/z$  calcd. for  $\text{C}_{11}\text{H}_{10}\text{Br}_5\text{N}_2^{+}$  568.6715, found 568.6274.

**5c** from **2c** was purified by crystallization from methanol. White crystals; Yield 87%; Mp.  $101\text{--}102^{\circ}\text{C}$ ; MS  $[\text{M}+\text{H}]^{+}$   $m/z$  calcd. for  $\text{C}_{11}\text{H}_{10}\text{Br}_4\text{N}_5^{+}$  531.7624, found 531.7014.

**8c** from **5c**; the product was purified by column chromatography (DCM/MeOH/TEA, 9/1/0.5 – 8/2/0.5) to afford **8c** as white solid. Yield 86%; Mp.  $120\text{--}122^{\circ}\text{C}$ ; FTMS  $[\text{M}+\text{H}]^{+}$   $m/z$  calcd. for  $\text{C}_{11}\text{H}_{12}\text{Br}_4\text{N}_3^{+}$  505.7718, found 505.7714;  $^1\text{H}$  NMR (500 MHz,  $\text{DMSO}-d_6$ )  $\delta$  ppm: 1.29–1.35 (m, 2H), 1.76–1.82 (m, 2H), 2.53 (t, 2H,  $J = 6.9$ ), 4.47 (t, 2H,  $J = 7.3$ ), 8.49 (s, 1H);  $^{13}\text{C}$  NMR (125 MHz,  $\text{DMSO}-d_6$ )  $\delta$  ppm: 29.53, 30.01, 41.41, 46.86, 107.01, 116.99, 120.80, 122.80, 131.71, 144.12, 149.31.

#### 4.1.3.4. 5-(4,5,6,7-Tetrabromo-1H-benzimidazol-1-yl)pentan-1-amine (**8d**).

From **1a**, after work-up and purification by column chromatography (DCM) **2d** was obtained as a white solid; yield 79%; Mp.  $111\text{--}114^{\circ}\text{C}$ ; MS  $[\text{M}+\text{H}]^{+}$   $m/z$  calcd. for  $\text{C}_{12}\text{H}_{12}\text{Br}_5\text{N}_2^{+}$  582.6871, found 582.6476.

**5d** from **2d** was purified by column chromatography (DCM/MeOH, 0-2% MeOH) to afford white solid, yield 68%; Mp. 148-149°C; MS  $[M+H]^+$   $m/z$  calcd. for  $C_{12}H_{12}Br_4N_5^+$  545.7780, found 545.7087.

**8d** from **5d**; the product was purified by column chromatography (DCM/MeOH/TEA, 9/1/0.5 – 8/2/0.5) to afford **8d** as a white solid. Yield 87%, Mp. 144-147°C; FTMS  $[M+H]^+$   $m/z$  calcd. for  $C_{12}H_{14}Br_4N_3^+$  519.7875, found 519.7876;  $^1H$  NMR (500 MHz, DMSO- $d_6$ )  $\delta$  ppm: 1.24-1.31 (m, 2H), 1.32-1.39 (m, 2H), 1.73-1.81 (m, 2H), 2.49 – 2.52 (m, 2H), 4.46 (t, 2H,  $J = 7.3$ ), 8.49 (s, 1H);  $^{13}C$  NMR (125 MHz, DMSO- $d_6$ )  $\delta$  ppm: 23.52, 31.90, 32.81, 41.71, 46.92, 107.02, 116.99, 120.81, 131.73, 144.13, 149.32.

#### 4.1.3.5. 4-(4,5,6,7-Tetrabromo-1H-benzotriazol-1-yl)butan-1-amine (**9c**).

From **1b**; after work-up and purification by column chromatography (hexane:DCM, 40-70% DCM) **3c** was obtained as a white solid, yield 14%; Mp. 89-91°C; MS  $[M+H]^+$   $m/z$  calcd. for  $C_{10}H_9Br_5N_3^+$  569.6667, found 569.6144.

**6c** from **3c**; the product was purified by crystallization from methanol/chloroform 10/1, affording **6c** as white crystals, yield 65%; Mp. 92-93°C; MS  $[M+H]^+$   $m/z$  calcd. for  $C_{10}H_9Br_4N_6^+$  532.7576, found 532.7770.

**9c** from **6c**; the product was purified by column chromatography (DCM/MeOH/TEA, 100/7/0.6) to afford **9c** as white solid, yield 52%; Mp. >211°C decomp.; MS  $[M+H]^+$   $m/z$  calcd. for  $C_{10}H_{11}Br_4N_4^+$  506.7671, found 506.7355;  $^1H$  NMR (500 MHz, DMSO- $d_6$ )  $\delta$  ppm: 1.49-1.64 (m, 2H), 1.90-2.06 (m, 2H), 2.70-2.87 (m, 2H), 4.93 (t, 2H,  $J = 6.8$  Hz);  $^{13}C$  NMR (125 MHz, DMSO- $d_6$ )  $\delta$  ppm: 24.35, 27.97, 38.58, 49.87, 107.34, 116.19, 124.02, 132.13, 145.39.

#### 4.1.3.6. 5-(4,5,6,7-Tetrabromo-1H-benzotriazol-1-yl)pentan-1-amine (**9d**).

From **1b**; after work-up and purification by column chromatography (hexane:DCM, 40-70% DCM) **3d** was obtained as white solid, yield 20%; Mp. 104-106°C; MS  $[M+H]^+$   $m/z$  calcd. for  $C_{11}H_{11}Br_5N_3^+$  585.6803, found 585.6236.

**6d** from **3d**; the product was purified by column chromatography (hexane/DCM, DCM 70-100%), affording **6d** as a white solid, yield 53%; Mp. 81-83°C; MS  $[M+H]^+$   $m/z$  calcd. for  $C_{11}H_{11}Br_4N_6^+$  546.7733, found 546.7888.

**9d** from **6d**; the product was purified by column chromatography (DCM/MeOH/TEA, 100/7/0.6) to afford **9d** as a white solid, yield 44%; Mp. >266°C decomp.; FTMS  $[M+H]^+$   $m/z$  calcd. for  $C_{11}H_{13}Br_4N_4^+$  520.7827, found 520.7829;  $^1H$  NMR (500 MHz, DMSO- $d_6$ )  $\delta$  ppm:

1.31-1.42 (m, 2H), 1.55-1.67 (m, 2H), 1.85-2.00 (m, 2H), 2.58 - 2.66 (m, 2H), 4.89 (t, 2H, J = 7.1 Hz);  $^{13}\text{C}$  NMR (125 MHz, DMSO- $d_6$ )  $\delta$  ppm: 23.01, 26.78, 30.53, 38.83, 50.10, 107.36, 116.18, 123.95, 132.10, 145.37.

#### 4.1.3.7. 3-(4,5,6,7-Tetrabromo-2H-benzotriazol-2-yl)propan-1-amine (**10b**).

From **7b**; the product was purified by column chromatography (DCM/MeOH/TEA, 80/2.5/0.4) to afford **10b** as a white solid, yield 68%; Mp. >242°C decomp.; FTMS  $[\text{M}+\text{H}]^+$   $m/z$  calcd. for  $\text{C}_9\text{H}_9\text{Br}_4\text{N}_4^+$  492.7514, found 492.7517;  $^1\text{H}$  NMR (500 MHz, DMSO- $d_6$ )  $\delta$  ppm: 2.18 (quin, 2H, J = 6.9 Hz), 2.72 (t, 2H, J = 6.9 Hz), 4.88 (t, 2H, J = 6.9 Hz);  $^{13}\text{C}$  NMR (125 MHz, DMSO- $d_6$ )  $\delta$  ppm: 31.07, 37.99, 55.13, 114.01, 125.97, 142.97.

#### 4.1.3.8. 4-(4,5,6,7-Tetrabromo-2H-benzotriazol-2-yl)butan-1-amine (**10c**).

From **1b**; after work-up and purification by column chromatography (hexane:DCM, 40-70% DCM) **4c** was obtained as a white solid, yield 43%; Mp. 155-156°C.

**7c** from **4c**; the product was purified by crystallization from methanol/chloroform 10/1, affording **7c** as a white crystals, yield 88%; Mp. 106-108°C.

**10c** from **7c**; the product was purified by column chromatography (DCM/MeOH/TEA, 80/2.5/0.4) to afford **10c** as a white solid; yield 84%; Mp. >264°C decomp.; FTMS  $[\text{M}+\text{H}]^+$   $m/z$  calcd. for  $\text{C}_{10}\text{H}_{11}\text{Br}_4\text{N}_4^+$  506.7671, found 506.7670;  $^1\text{H}$  NMR (500 MHz, DMSO- $d_6$ )  $\delta$  ppm: 1.35 – 1.50 (m, 2H), 2.06 (quin, 2H, J = 7.3 Hz), 2.64 (t, 2H, J = 6.9 Hz), 4.80 (t, 2H, J = 7.1 Hz);  $^{13}\text{C}$  NMR (125 MHz, DMSO- $d_6$ )  $\delta$  ppm: 27.12, 28.28, 57.26, 114.01, 125.96, 142.94.

#### 4.1.3.9. 5-(4,5,6,7-Tetrabromo-2H-benzotriazol-2-yl)pentan-1-amine (**10d**).

From **1b**; after work-up and purification by column chromatography (hexane:DCM, 40-70% DCM) **4d** was obtained as a white solid, yield 63%; Mp. 163-164°C.

**7d** from **4d**; the product was purified by crystallization from methanol/chloroform 10/1, affording **7d** as a white crystals, yield 90%; Mp. 88-90°C.

**10d** from **7d**; the product was purified by column chromatography (DCM/MeOH/TEA, 95/5/0.5) to afford **10d** as a white solid, yield 93%; Mp. 232-235°C; FTMS  $[\text{M}+\text{H}]^+$   $m/z$  calcd. for  $\text{C}_{11}\text{H}_{13}\text{Br}_4\text{N}_4^+$  520.7827, found 520.7828;  $^1\text{H}$  NMR (500 MHz, DMSO- $d_6$ )  $\delta$  ppm: 1.24 – 1.41 (m, 2H), 1.47 – 1.65 (m, 2H), 1.90 – 2.14 (m, 2H), 2.73 (t, 2H, J = 7.3 Hz); 4.79 (t, 2H, J = 6.8);  $^{13}\text{C}$  NMR (125 MHz, DMSO- $d_6$ )  $\delta$  ppm: 23.15, 26.84, 29.05, 38.87, 57.23, 114.04, 125.95, 142.97.

4.1.3.10. 2-(4,5,6,7-Tetrabromo-2-methyl-1H-benzimidazol-1-yl)ethan-1-amine (**14a**).

From **11**; after work-up and purification by column chromatography (DCM) **12a** was obtained as a white solid; yield 29%; Mp. 174-176°C; MS  $[M+H]^+$   $m/z$  calcd. for  $C_{10}H_8Br_5N_2^+$  554.6558, found 554.6149.

**13a** from **12a**; the product was purified by crystallization from methanol affording **13a** as a white crystals; yield 96%; Mp. 173-177°C; MS  $[M+H]^+$   $m/z$  calcd. for  $C_{10}H_8Br_4N_5^+$  517.7467, found 517.7076;

**14a** from **13a**; the product was purified by column chromatography (DCM/MeOH/TEA, 9/1/0.5) to afford **14a** as a white solid, yield 70%; Mp. 149-152°C; FTMS  $[M+H]^+$   $m/z$  calcd. for  $C_{10}H_{10}Br_4N_3^+$  491.7562, found 491.7564;  $^1H$  NMR (500 MHz, DMSO- $d_6$ )  $\delta$  ppm: 2.60 (s, 3H), 2.89 (t, 2H, J = 6.6), 4.35 (t, 2H, J = 6.6 Hz);  $^{13}C$  NMR (125 MHz, DMSO- $d_6$ )  $\delta$  ppm: 15.09, 43.24, 48.11, 106.31, 115.65, 120.18, 121.77, 132.62, 157.76.

4.1.3.11. 3-(4,5,6,7-Tetrabromo-2-methyl-1H-benzimidazol-1-yl)propan-1-amine (**14b**).

From **11**; after work-up and purification by column chromatography (DCM) product **12b** was obtained as a mixture of 4,5,6,7-tetrabromo-1-(3-chloropropyl)-2-methyl-1H-benzimidazole and 4,5,6,7-tetrabromo-1-(3-bromopropyl)-2-methyl-1H-benzimidazole; MS  $[M+H]^+$   $m/z$  calcd. for  $C_{11}H_{10}Br_4ClN_2^+$  524.7220, found 524.6685 and  $C_{11}H_{10}Br_5N_2^+$  568.6715, found 568.6478 and was used without further purification.

**13b** from **12b**; the product was purified by crystallization from methanol affording **13b** as a white solid, yield 37% from **11**; Mp. 168-170°C; MS  $[M+H]^+$   $m/z$  calcd. for  $C_{11}H_{10}Br_4N_5^+$  531.7624, found 531.7864;

**14b** from **13b**; the product was purified by column chromatography (DCM/MeOH/TEA, 9/1/0.5) to afford **14b** as a white solid, yield 96%; Mp. >131°C decomp.; FTMS  $[M+H]^+$   $m/z$  calcd. for  $C_{11}H_{12}Br_4N_3^+$  505.7718, found 505.7717;  $^1H$  NMR (500 MHz, DMSO- $d_6$ )  $\delta$  ppm: 1.83-1.92 (m, 2H); 2.60 (s, 3H), 2.70 (t, 2H, J = 6.7), 4.47 (t, 2H, J = 6.7 Hz);  $^{13}C$  NMR (125 MHz, DMSO- $d_6$ )  $\delta$  ppm: 14.64, 33.43, 38.16, 52.48, 109.99, 115.73, 120.36, 121.97, 132.55, 143.16, 157.12.

4.1.3.12. 4-(4,5,6,7-Tetrabromo-2-methyl-1H-benzimidazol-1-yl)butan-1-amine (**14c**).

From **11**; after work-up and purification by column chromatography (DCM/MeOH 99/1) **12c** was obtained as a white solid; yield 59%; Mp. 148-152°C; MS  $[M+H]^+$   $m/z$  calcd. for  $C_{12}H_{12}Br_5N_2^+$  582.6871, found 582.6865;

**13c** from **12c**; the product was purified by crystallization from methanol affording **13c** as a white crystals, yield 99%; Mp. 90-95°C; MS  $[M+H]^+$   $m/z$  calcd. for  $C_{12}H_{12}Br_4N_5^+$  545.7780, found 545.7614;

**14c** from **13c**; the product was purified by column chromatography (DCM/MeOH/TEA, 9/1/0.5) to afford **14c** as a white solid, yield 64%; Mp. >112°C decomp.; FTMS  $[M+H]^+$   $m/z$  calcd. for  $C_{12}H_{14}Br_4N_3^+$  519.7875, found 519.7879;  $^1H$  NMR (500 MHz, DMSO- $d_6$ )  $\delta$  ppm: 1.40-1.54 (m, 2H), 1.66-1.83 (m, 2H), 2.53-2.71 (m, 5H), 4.25-4.48 (m, 2H);  $^{13}C$  NMR (125 MHz, DMSO- $d_6$ )  $\delta$  ppm: 14.62, 28.81, 29.00, 41.00, 52.47, 106.36, 115.74, 120.35, 122.01, 132.49, 143.11, 157.00.

#### 4.1.3.13. 5-(4,5,6,7-Tetrabromo-2-methyl-1H-benzimidazol-1-yl)pentan-1-amine (**14d**).

From **11**; after work-up and purification by column chromatography (DCM) **12d** was obtained as a white solid; yield 58%; Mp. 149-155°C; MS  $[M+H]^+$   $m/z$  calcd. for  $C_{13}H_{14}Br_5N_2^+$  596.7028, found 596.6276.

**13d** from **12d**; the product was purified by column chromatography (DCM) affording **13d** as a white solid; yield 99%; Mp. 117-120°C; MS  $[M+H]^+$   $m/z$  calcd. for  $C_{13}H_{14}Br_4N_5^+$  559.7937, found 559.7260;

**14d** from **13d**; the product was purified by column chromatography (DCM/MeOH/TEA, 9/1/0.5) to afford **14d** as a white solid; yield 86%, Mp. > 92°C decomp.; FTMS  $[M+H]^+$   $m/z$  calcd. for  $C_{13}H_{16}Br_4N_3^+$  533.8031, found 533.8032;  $^1H$  NMR (500 MHz, DMSO- $d_6$ )  $\delta$  ppm: 1.33-1.47 (m, 4H), 1.65-1.75 (m, 2H), 2.54 (t, 2H,  $J = 6.4$  Hz), 2.58 (s, 3H), 4.29-4.41 (m, 2H);  $^{13}C$  NMR (125 MHz, DMSO- $d_6$ )  $\delta$  ppm: 14.61, 23.58, 31.25, 32.66, 41.62, 52.47, 106.30, 115.73, 120.32, 121.97, 132.45, 143.10, 156.94.

## 4.2. Crystallization

### 4.2.1. CK2 Protein for crystallization

The C-terminal truncated version of human CK2 $\alpha$  (CK2 $\alpha^{1-335}$ ) was expressed and purified as described previously [23] with the exception that the P11 phosphocellulose chromatography step was replaced with a batch purification step using the same resin material. Purified CK2 $\alpha^{1-335}$  was rebuffed in storage solution (25 mM Tris/HCl, 500 mM NaCl, pH 8.5). The final CK2 $\alpha^{1-335}$  protein concentration was 7 mg/mL as determined via UV-absorption at 280 nm.

The CK2 $\alpha$ <sup>1-335</sup> solution (90  $\mu$ L) were mixed with 10  $\mu$ L of a 10 mM **8b** solution in DMSO. The mixture incubated for 30 min at room temperature; afterwards precipitated material was removed by centrifugation. CK2 $\alpha$ <sup>1-335</sup>/**8b** co-crystals were obtained in high-salt and in low-salt conditions using the sitting drop variant of vapor diffusion at 20°C. The optimized drop composition was 1  $\mu$ L of the preincubated CK2 $\alpha$ <sup>1-335</sup>/**8b** mixture and 1  $\mu$ L reservoir solution. The optimized reservoir solutions were 4.4 M NaCl, 0.1 M sodium acetate, pH 5.5, (high-salt case) and 25% (w/v) PEG3350, 0.2 M ammonium sulfate, 0.1 M BIS-TRIS buffer, pH 5.5 (low-salt case).

#### 4.2.2. X-Ray Diffractometry

Suitable CK2 $\alpha$ <sup>1-335</sup>/**8b** co-crystals were flash-frozen in liquid nitrogen. Cryo conditions for the low-salt CK2 $\alpha$ <sup>1-335</sup>/**8b** crystals were obtained by adding (R)-butane-1,3-diol into the drop. The high-salt condition was already a cryo condition. Preliminary X-ray diffraction data were collected at the beamline X06DA of the Swiss Light Source (SLS), Paul Scherrer Institut, in Villigen, Switzerland. The final diffraction data sets were obtained at the beamline ID23-1 of the European Synchrotron Radiation Facility (ESRF) in Grenoble, France, using wavelengths of 1 Å (high-salt structure) and 0.9660 Å (low-salt structure) and a temperature of 100 K. The diffraction data sets were integrated with XDS [37] and scaled with AIMLESS [38] from the CCP4 software suite [39].

#### 4.2.3. Structure Solution, Refinement, Validation, Deposition and Illustration

The complex structures were solved by molecular replacement with PHASER [40] using the protein chain of the CK2 $\alpha$ <sup>1-335</sup> structure 5CQU [41] as a search model. The structures were refined and validated using PHENIX [42] which also served to generate the topology of the **8b** molecule. COOT [43] was used for manual corrections of the structures. The final structures are available at the Protein Data Bank under the accession codes 5OWH (high-salt structure) and 5OWL (low-salt structure). The structure illustrations in Figure 2 were prepared with PYMOL [44].

### 4.3 Biological assays

#### 4.3.1. Cloning, expression and purification of human CK2 $\alpha$ and CK2 $\beta$ kinase

The coding regions of human CK2 $\alpha$  and CK2 $\beta$  were amplified by PCR using the following primers: 5'- CCG GAA TTC TCG GGA CCC GTG CCA AGC AGG (CK2 $\alpha$ F),

5'- TAA AGC GGC CGC TGC TGA GCG CCA GCG G (CK2 $\alpha$ R), 5'- GGA ATT CCA TAT GAG CAG CTC AGA GGA GGT GTC C-3' (CK2 $\beta$ F) and 5'- CCC AAG CTT CAA ACC CGT TTA GAG GCC C-3' (CK2 $\beta$ R) and IMAGE clones (GenBank entry BC053532.1 and BC112017.1) as a template. The CK2 $\alpha$  PCR-product was digested with EcoRI and NotI and ligated into pGEX4T1 vector (GE Healthcare) carrying a N-terminal GST tag. The CK2 $\beta$  PCR-product was digested with NdeI and HindIII and ligated into pET28a vector (Novagen) carrying a N-terminal His tag. The cloned CK2 $\alpha$  and CK2 $\beta$  genes were verified by sequencing.

GST-CK2 $\alpha$  and His-CK2 $\beta$  were overproduced separately in the bacterial strain BL21(DE3)pLysS (Invitrogen) growing in Super Broth medium [13] after induction with 1 mM IPTG for 20 h at 20°C. Pellets were resuspended in extraction buffer (20 mM NaH<sub>2</sub>PO<sub>4</sub>, pH 7.9) 500 mM NaCl, 50 mM imidazole, protease inhibitors (Complete EDTA-free, Roche), mixed (2:1 pellet  $\alpha$ : $\beta$  mass ratio) and sonicated. The cleared lysate was loaded onto HisTrap HP 5 mL column mounted on a AKTA Purifier 10 FPLC system (GE Healthcare). CK2 holoenzyme was eluted with imidazole gradient in extraction buffer (50-500 mM). Fractions containing His-tagged CK2 were dialyzed against 20 mM NaH<sub>2</sub>PO<sub>4</sub> (pH 7.9), 200 mM NaCl and loaded onto GSTTrap HP 5 mL column (GE Healthcare). GST-tagged CK2 was eluted with 10 mM glutathione in dialysis buffer. Finally, fractions containing CK2 holoenzyme were dialyzed overnight against 25 mM Tris-HCl pH 8.5, 200 mM NaCl, 1 mM DTT, 0-25% glycerol and stored at -20°C. The protein concentration in final solution was 1.61 mg/mL (determined by Bradford method with bovine serum albumin as a standard) [45].

#### 4.3.2. Cloning, expression and purification of human kinase PIM1

The coding region of human PIM1 was amplified by PCR using the following primers: 5'- GGA ATT CCA TAT GCT CTT GTC CAA AAT CAA CTC GCT TG (PIM1F) and 5'- CAA GCT TGT TTG CTG GGC CCC GGC GA (PIM1R) and IMAGE clone (GenBank entry BC0020224.1) as a template. The PIM1 PCR-product was digested with NdeI and HindIII and ligated into pET28a vector (Novagen) carrying a N-terminal His tag. The cloned PIM1 gene was verified by sequencing.

Expression of N-terminal histidine-tagged PIM1 was done in the bacterial strain BL21(DE3)pLysS (Invitrogen) growing in Super Broth medium after induction with 1 mM IPTG for 20 h at 20°C. The cell pellet from 800 mL of bacterial culture was resuspended in extraction buffer (20 mM Tris-HCl pH 8.0, 150 mM NaCl, 20 mM imidazole, protease

inhibitors (Complete EDTA-free, Roche)) and sonicated. The cleared lysate was loaded onto HisTrap HP 5 mL column mounted on a AKTA Purifier 10 FPLC system (GE Healthcare). PIM1 was eluted with imidazole gradient in extraction buffer (20-500 mM). Fractions containing His-tagged PIM1 were dialysed against 50 mM Tris-HCl pH 7.5, 150 mM NaCl, 2 mM DTT, 0.5 mM PMSF, 0-25% glycerol and stored at -20°C. The protein concentration in final solution was 3.0 mg/mL (determined by Bradford method with bovine serum albumin as a standard) [45].

#### 4.3.3. Phosphorylation assays

The new TBBi and TBBt derivatives were tested for their inhibitory activity toward human CK2 $\alpha$ , human CK2 holoenzyme and PIM1 (Table 3) using P81 filter isotopic assay [46]. CK2 $\alpha$  activity was tested in final volume of 50  $\mu$ L containing CK2 $\alpha$  (21.2 nM), Tris-HCl (pH 7.5; 23 mM), MgCl<sub>2</sub> (20 mM), DTT (0.4 mM), synthetic peptide substrate (RRRADDSDDDDD 40  $\mu$ M; Biaffin GmbH), [ $\gamma$ -<sup>32</sup>P]-ATP (10  $\mu$ M, 200-300 cpm/pmol) and appropriate concentrations of inhibitor in 2  $\mu$ L DMSO or 2  $\mu$ L DMSO as control. After 15 min incubation at 30°C, 5  $\mu$ L of the assay mixture was spotted onto P81 paper, which was subsequently washed with 0.6% *o*-phosphoric acid three times and allowed to dry.

CK2 holoenzyme activity was tested in final volume of 50  $\mu$ L containing CK2 holoenzyme (28.6 nM), Tris-HCl (pH 7.5, 23 mM), NaCl (100 mM), MgCl<sub>2</sub> (20 mM), DTT (0.4 mM), peptide substrate RRRADDSDDDDD (40  $\mu$ M) and [ $\gamma$ -<sup>32</sup>P]-ATP (20  $\mu$ M, 200-300 cpm/pmol) and appropriate concentrations of inhibitor in 2  $\mu$ L DMSO or 2  $\mu$ L DMSO as control. The reaction mixture was incubated for 15 min at 30°C, and treated as above.

PIM1 activity was tested in final volume of 50  $\mu$ L containing PIM1 (25.30 nM), Tris-HCl (pH 7.5, 23 mM), MgCl<sub>2</sub> (20 mM), DTT (0.4 mM), [ $\gamma$ -<sup>32</sup>P]-ATP (20  $\mu$ M, 200-300 cpm/pmol), and 30  $\mu$ M synthetic peptide substrate ARKRRRHPSGPPTA. The reaction was initiated with enzyme, incubated for 20 min at 30°C, and next 5  $\mu$ L of the reaction mixture was spotted onto P81 paper. The filter papers were washed 3 x with 0.6% *o*-phosphoric acid and once with 95% ethanol before counting in a scintillation counter (Canberra-Packard).

The IC<sub>50</sub> values for studied compounds were determined at 4% DMSO with 8 concentrations of each tested inhibitor at the range of 0.064-1000  $\mu$ M and calculated by fitting the data to sigmoidal dose-response (variable slope)  $Y = \text{Bottom} + (\text{Top}-\text{Bottom}) / (1+10^{((\text{LogIC}_{50}-X)*\text{HillSlope})})$  equation in GraphPad Prism.

#### 4.3.4 Selectivity profile

Specificity studies for compounds **8b** and **14b** at 5  $\mu\text{M}$  concentration were performed in ProQinase GmbH, Freiburg, Germany.

#### 4.3.5 Cell culture and treatment

CCRF-CEM (human Caucasian acute lymphoblastic leukemia, ECACC 85112105) were obtained from ECACC, MCF-7 (human breast cancer cell line, authentication certificate, ATCC STRA4788) was a gift from Nencki Institute of Experimental Biology in Warsaw, PAS. PC-3 (human prostate cancer) was a gift from National Medicines Institute, Warsaw, Poland. MCF-7 were cultured in DMEM with high glucose medium (Lonza) with 10  $\mu\text{g}/\text{mL}$  of human recombinant insulin. CCRF-CEM suspension cells and PC-3 cells were cultured in RPMI 1640 medium (Lonza). All cell lines were supplemented with 10% fetal bovine serum (EuroClone), 2 mM L-glutamine and antibiotics (100 U/mL penicillin, 100  $\mu\text{g}/\text{mL}$  streptomycin) and grown in 75  $\text{cm}^2$  cell culture flasks (Sarstedt), in a humidified atmosphere of  $\text{CO}_2/\text{air}$  (5/95%) at 37°C.

#### 4.3.6 Cell viability assays (MTT-based) and $\text{EC}_{50}$ determination

Before the treatment, adherent cells (MCF-7, and PC-3) were trypsinized in 0.25% trypsin-EDTA solution (Sigma-Aldrich) and seeded into 96-well microplates at  $0.6 \times 10^4$  cells/well. CCRF-CEM were seeded at  $2 \times 10^4$  cells/well. Leukemia cells after seeding and adherent cells 24 h after plating (at 70% of confluency) were treated with tested compounds at the appropriate concentrations or DMSO at 0.5% final concentration.  $\text{EC}_{50}$  values were determined at eight concentrations in the range of 0.39-50  $\mu\text{M}$  for each inhibitor for PC-3, and 0.78-100  $\mu\text{M}$  for MCF-7 and 1.2-20  $\mu\text{M}$  or 0.1-2.0  $\mu\text{M}$  (**14a**) for CCRF-CEM. The experimental data were fitted to sigmoidal dose-response (variable slope)  $Y = \text{Bottom} + (\text{Top} - \text{Bottom}) / (1 + 10^{((\text{LogIC}_{50} - X) * \text{HillSlope}))}$  equation in GraphPad Prism.

After 48 h incubation with compounds or DMSO, suspension cells were centrifuged and supernatants of CCRF-CEM, MCF-7 and PC-3 cells were discarded; subsequently MTT stock solution (Sigma-Aldrich) was added to each well to a final concentration of 0.5 mg/mL. After 2 h of incubation at 37°C, water-insoluble dark blue formazan crystals were dissolved in DMSO (200  $\mu\text{L}$ ) (37°C/10 min incubation). Optical densities were measured at 570 nm using BioTek microplate reader. All measurements were carried out in triplicate and the results are expressed in percentage of cell viability relative to control (cells without inhibitor in 0.5% DMSO).

**Supplementary Materials:** HRMS spectra,  $^1\text{H}$ -NMR, and  $^{13}\text{C}$ -NMR spectra are available online at

### Declaration of interest

The authors report no conflicts of interest.

**Acknowledgments:** This work was supported by an NSC Poland grant 2014/13/B/NZ7/02273, by Warsaw University of Technology and by the Deutsche Forschungsgemeinschaft (grant NI 643/4-2).

We thank the staff of the beamline X06DA at the SLS (Villigen, Switzerland) and of the beamline ID23-1 at the ESRF (Grenoble, France) for support with X-ray data collection. We are grateful to Professor Ulrich Baumann (University of Cologne) for access to protein crystallography infrastructure.

---

### References

- [1] C.E. Ortega, Y. Seidner, I. Dominguez, Mining CK2 in Cancer, PLoS ONE. 9 (2014) e115609, doi:10.1371/journal.pone.0115609
- [2] Y. Tursynbay, J. Zhang, Z. Li, T. Tokay, Z. Zhumadilov, D. Wu, Y. Xie, Pim-1 kinase as cancer drug target: An update, Biomed. Rep. 4 (2016), 140-146
- [3] R. Romieu-Mourez, E. Landesman-Bollag, D.C. Seldin, A.M. Traish, F. Mercurio, G.E. Sonenshein, Roles of IKK Kinases and Protein Kinase CK2 in Activation of Nuclear Factor- $\kappa\text{B}$  in Breast Cancer, Cancer Res. 61 (2001) 3810-3818
- [4] P.S. Hammerman, C.J. Fox, R.M. Cinalli, A. Xu, J.D. Wagner, T. Lindsten, C.B. Thompson, Lymphocyte transformation by Pim-2 is dependent on nuclear factor- $\kappa\text{B}$  activation, Cancer Res. 64 (2004) 8341-8348.
- [5] G.K. Gray, B.C. McFarland, A.L. Rowse, S.A. Gibson, E.N. Benveniste, Therapeutic CK2 inhibition attenuates diverse prosurvival signaling cascades and decreases cell viability in human breast cancer cells, Oncotarget 5 (2014) 6484-6496

- [6] M. Koronkiewicz, Z. Chilmończyk, Z. Kazimierczuk, A. Orzeszko, Deoxynucleosides with benzimidazoles as aglycone moiety are potent anticancer agents, *Eur. J. Pharmacol.* 820 (2018) 146-155
- [7] B.H. Naguib, H.B. El-Nassan, T.M. Abdelghany, Synthesis of new pyridothienopyrimidinone derivatives as Pim-1 inhibitors, *J. Enzyme Inhib. Med. Chem.* 32 (2017) 457-467
- [8] A.L. Merkel, E. Meggers, M. Ocker, PIM1 kinase as a target for cancer therapy, *Expert Opin. Investig. Drugs* 4 (2012) 425-36
- [9] G.M. Arunesh, E. Shanthi, M.H. Krishna, J Sooriya Kumar, V.N. Viswanadhan, Small molecule inhibitors of PIM1 kinase: July 2009 to February 2013 patent update, *Expert Opin. Ther. Pat.* 1 (2014) 5-17
- [10] L.S. Chen, S. Redkar, D. Bearss, W.G. Wierda, V. Gandhi, Pim kinase inhibitor, SGI-1776, induces apoptosis in chronic lymphocytic leukemia cells, *Blood* 114 (2009) 4150–4157
- L.S. Chen, S. Redkar, P. Taverna, J.E. Cortes, V. Gandhi, Mechanisms of cytotoxicity to Pim kinase inhibitor, SGI-1776, in acute myeloid leukemia, *Blood* 118 (2011) 693–702
- [11] M.T. Burger, G. Nishiguchi, W. Han, J. Lan, R. Simmons, G. Atallah, Y. Ding, V. Tamez, Y. Zhang, M. Mathur, K. Muller, C. Bellamacina, M.K. Lindvall, R. Zang, K. Huh, P. Feucht, T. Zavorotinskaya, Y. Dai, S. Basham, J. Chan, E. Ginn, A. Aycinena, J. Holash, J. Castillo, J.L. Langowski, Y. Wang, M.Y. Chen, A. Lambert, C. Fritsch, A. Kauffmann, E. Pfister, K.G. Vanasse, P.D. Garcia, Identification of N-(4-((1R,3S,5S)-3-Amino-5-methylcyclohexyl)pyridin-3-yl)-6-(2,6-difluorophenyl)-5-fluoropicolinamide (PIM447), a Potent and Selective Proviral Insertion Site of Moloney Murine Leukemia (PIM) 1, 2, and 3 Kinase Inhibitor in Clinical Trials for Hematological Malignancies, *J. Med. Chem.* 58 (2015) 8373-86
- [12] E.K. Keeton, K. McEachern, K.S. Dillman, S. Palakurthi, Y. Cao, M.R. Grondine, S. Kaur, S. Wang, Y. Chen, A. Wu, M. Shen, F.D. Gibbons, M.L. Lamb, X. Zheng, R.M. Stone, D.J. DeAngelo, L.C. Plataniias, L.A. Dakin, H. Chen, P.D. Lyne, D. Huszar, AZD1208, a potent and selective pan-Pim kinase inhibitor, demonstrates efficacy in preclinical models of acute myeloid leukemia, *Blood* 123 (2014) 905–913
- [13] A. Gianoncelli, G. Cozza, A. Orzeszko, F. Meggio, Z. Kazimierczuk, L.A. Pinna, Tetraiodobenzimidazoles are potent inhibitors of protein kinase CK2, *Bioorg. Med. Chem.* 17 (2009) 7281-7289

- [14] G. Cozza, C. Girardi, A. Ranchio, G. Lolli, S. Sarno, A. Orzeszko, Z. Kazimierczuk, R. Battistutta, M. Ruzzene, L.A. Pinna, Cell- permeable dual inhibitors of protein kinases CK2 and PIM- 1: structural features and pharmacological potential, *Cell. Mol. Life Sci.* 71 (2014) 3173-3185
- [15] K. Chojnacki, P. Wińska, K. Skierka, M. Wielechowska, M. Bretner, Synthesis, *in vitro* antiproliferative activity and kinase profile of new benzimidazole and benzotriazole derivatives, *Bioorg. Chem.* 72 (2017) 1–10
- [16] M. Lopez-Ramos, R. Prudent, V. Moucadel, C.F. Sautel, C. Barette, L. Lafanechere, L. Mouawad, D. Grierson, F. Schmidt, J.C. Florent, P. Filippakopoulos, A.N. Bullock, S. Knapp, J.B. Reiser, C. Cochet, New potent dual inhibitors of CK2 and PIM kinases: discovery and structural insights, *FaSeB J.* 24 (2010) 3171–3185
- [17] A. Siddiqui-Jain, D. Drygin, N. Streiner, P. Chua, F. Pierre, S.E. O'Brien, J. Bliesath, M. Omori, N. Huser, C. Ho, Ch. Proffitt, M.K. Schwaebe, D.M. Ryckman, W.G. Rice, K. Anderes, CX-4945, an Orally Bioavailable Selective Inhibitor of Protein Kinase CK2, Inhibits Prosurvival and Angiogenic Signaling and Exhibits Antitumor Efficacy, *Cancer Res.* 70 (2010) 10288-10298
- [18] F. Pierre, C.F. Regan, M.C. Chevrel, A.Siddiqui-Jain, D. Macalino, N. Streiner, D. Drygin, M. Haddach, S.E. O'Brien, W.G. Rice, D. M. Ryckman, Novel potent dual inhibitors of CK2 and Pim kinases with antiproliferative activity against cancer cells, *Bioorg. Med. Chem. Lett.* 22 (2012) 3327–3331
- [19] E. Łukowska-Chojnacka, P. Winska, M. Wielechowska, M. Poprzeczko, M. Bretner , Synthesis of novel polybrominated benzimidazole derivatives — potential CK2 inhibitors with anticancer and proapoptotic activity, *Bioorg. Med. Chem.* 24 (2016) 735–741
- [20] Y. Cheng, W.H. Prusoff, Relationship between the inhibition constant ( $K_i$ ) and the concentration of inhibitor which causes 50 percent inhibition ( $IC_{50}$ ) of an enzymatic reaction, *Biochem. Pharmacol.* 22 (1973) 3099–3108.]
- [21] M.A. Pagano, J. Bain, Z. Kazimierczuk, S. Sarno, M. Ruzzene, G. Di Maira, M. Elliott, A. Orzeszko, G. Cozza, F. Meggio, L.A. Pinna, The selectivity of inhibitors of protein kinase CK2: an update, *Biochem. J.* 415 (2008) 353–365
- [22] R. Battistutta, G. Cozza, F. Pierre, E. Papinutto, G. Lolli, S. Sarno, S.E. O'Brien, Adam Siddiqui-Jain, M. Haddach, K. Anderes, D.M. Ryckman, F. Meggio, L.A. Pinna,

- Unprecedented Selectivity and Structural Determinants of a New Class of Protein Kinase CK2 Inhibitors in Clinical Trials for the Treatment of Cancer, *Biochemistry* 50 (2011) 8478–8488
- [23] I. Ermakova, B. Boldyreff, O. Issinger, K. Niefind, Crystal structure of a C-terminal deletion mutant of human protein kinase CK2 catalytic subunit. *J. Mol. Biol.* 330 (2003) 925-934
- [24] K. Niefind, N. Bischoff, A.G. Golub, V.G. Bdzhola, A.O. Balanda, A.O. Prykhod'ko, S.M. Yarmoluk, Structural Hypervariability of the Two Human Protein Kinase CK2 Catalytic Subunit Paralogs Revealed by Complex Structures with a Flavonol- and a Thieno[2,3-d]pyrimidine-Based Inhibitor. *Pharmaceuticals* 10, (2017) 9, doi: 10.3390/ph10010009
- [25] B. Guerra, N. Bischoff, V.G. Bdzhola, S.M. Yarmoluk, O.G. Issinger, A.G. Golub, K. Niefind, A Note of Caution on the Role of Halogen Bonds for Protein Kinase/Inhibitor Recognition Suggested by High- And Low-Salt CK2 $\alpha$  Complex Structures. *ACS Chem. Biol.* 10 (2015) 1654-1660
- [26] R. Battistutta, E. De Moliner, S. Sarnó, G. Zanotti, L.A. Pinna, Structural features underlying selective inhibition of protein kinase CK2 by ATP site-directed tetrabromo-2-benzotriazole. *Protein. Sci.* 10, (2001) 2200-2206
- [27] C.W. Yde, I. Ermakova, O.G. Issinger, K. Niefind, Inclining the purine base binding plane in protein kinase CK2 by exchanging the flanking side-chains generates a preference for ATP as a cosubstrate. *J. Mol. Biol.* 347 (2005) 399-414
- [28] J. Raaf, E. Brunstein, O. Issinger, K. Niefind, The CK2 $\alpha$ /CK2 $\beta$  interface of human protein kinase CK2 harbors a binding pocket for small molecules. *Chem. Biol.* 15 (2008) 111-117
- [29] K. Niefind, O.G. Issinger, Conformational plasticity of the catalytic subunit of protein kinase CK2 and its consequences for regulation and drug design. *Biochim. Biophys. Acta* 1804 (2010) 484-492
- [30] K. Klopffleisch, O.G. Issinger, K. Niefind, Low-density crystal packing of human protein kinase CK2 catalytic subunit in complex with resorufin or other ligands: a tool to study the unique hinge-region plasticity of the enzyme without packing bias. *Acta Cryst. D* 68 (2012) 883-892
- [31] N. Bischoff, J. Raaf, B. Olsen, M. Bretner, O.G. Issinger, K. Niefind, Enzymatic activity with an incomplete catalytic spine: insights from a comparative structural analysis of

- human CK2 alpha and its paralogous isoform CK2 alpha'. *Mol. Cel. Bioch.* 356, (2011) 57-65
- [32] D. Liebschner, P.V. Afonine, N.W. Moriarty, B.K. Poon, O.V. Sobolev, T.C. Terwilliger, P.D. Adams, Polder maps: improving OMIT maps by excluding bulk solvent, *Acta Cryst. D* 73 (2017) 148-157
- [33] Y. Lu, Y. Wang, W. Zhu, Nonbonding interactions of organic halogens in biological systems: implications for drug discovery and biomolecular design, *Phys. Chem. Chem. Phys.* 12 (2010) 4543-4551
- [34] H. Matter, M. Nazaré, S. Güssregen, D.W. Will, H. Schreuder, A. Bauer, M. Urmann, K. Ritter, M. Wagner, V. Wehner, Evidence for C-Cl/C-Br... $\pi$  interactions as an important contribution to protein-ligand binding affinity, *Angew. Chem. Int. Ed. Engl.* 48 (2009) 2911-2916
- [35] N. Bischoff, B. Olsen, J. Raaf, M. Bretner, O.G. Issinger, K. Niefind, Structure of the human protein kinase CK2 catalytic subunit CK2 $\alpha'$  and interaction thermodynamics with the regulatory subunit CK2 $\beta$ , *J. Mol. Biol.* 407 (2011) 1-12.
- [36] A. Najda-Bernatowicz, M. Łebska, A. Orzeszko, K. Kopańska, E. Krzywińska, G. Muszyńska, M. Bretner, Synthesis of new analogs of benzotriazole, benzimidazole and phthalimide - potential inhibitors of human protein kinase CK2, *Bioorg. Med. Chem.* 17 (2009) 1573-1578
- [37] W. Kabsch, XDS. *Acta Cryst. D* 66 (2010) 125-132
- [38] P.R. Evans, G.N. Murshudov, How good are my data and what is the resolution?, *Acta Cryst. D* 69 (2013) 1204-1214
- [39] M.D. Winn, C.C. Ballard, K.D. Cowtan, E.J. Dodson, P. Emsley, P.R. Evans, R.M. Keegan, E.B. Krissinel, A.G.W. Leslie, A. McCoy, S.J. McNicholas, G.N. Murshudov, N.S. Pannu, E.A. Potterton, H.R. Powell, R.J. Read, A. Vagin, K.S. Wilson, Overview of the CCP4 suite and current developments, *Acta Cryst. D* 67 (2011) 235-242
- [40] A.J. McCoy, R.W. Grosse-Kunstleve, P.D Adams, M.D. Winn, L.C. Storoni, R.J. Read, Phaser crystallographic software, *J. Appl. Crystallogr.* 40 (2007) 658-674
- [41] R. Swider, M. Maslyk, J.M. Zapico, C. Coderch, R. Panchuk, N. Skorokhyd, A. Schnitzler, K. Niefind, B. de Pascual-Teresa, A. Ramos, Synthesis, biological activity and structural study of new benzotriazole-based protein kinase CK2 inhibitors, *RSC Advances* 5 (2015) 72482-72494

- 
- [42] P.D. Adams, P.V. Afonine, G. Bunkóczi, V.B. Chen, I.W. Davis, N. Echols, J.J. Headd, L.W. Hung, G.J. Kapral, R.W. Grosse-Kunstleve, A.J. McCoy, N.W. Moriarty, R. Oeffner, R.J. Read, D.C. Richardson, J.S. Richardson, T.C. Terwilliger, P.H. Zwart, PHENIX: a comprehensive Python-based system for macromolecular structure solution, *Acta Cryst. D* 66 (2010) 213-221
- [43] P. Emsley, B. Lohkamp, W.G. Scott, K. Cowtan, Features and development of Coot, *Acta Cryst. D* 66 (2010) 486-501
- [44] The PyMOL Molecular Graphics System ed. Schrödinger, LLC (2013)
- [45] M.M. Bradford, A rapid and sensitive method for the quantification of microgram quantities of protein utilising the principle of protein-dye binding, *Anal. Biochem.* 72 (1976) 248-254
- [46] S. Sarno, P. Vaglio, F. Meggio, O.-G. Issinger, L.A. Pinna, Protein kinase CK2 mutants defective in substrate recognition, *J. Biol. Chem.* 271 (1996) 10595–10601

---

### Highlights

A series of new alkylamino- TBBi and TBBt derivatives were synthesized

The novel aminoalkyl- TBBi derivatives **8b-c** inhibit the activity of protein kinases: CK2 holoenzyme and the PIM1 as effectively as TBBi, while the derivatives of 2MeTBBi, compounds **14a-b** exerted superior inhibition of PIM1 kinase.

New aminoalkyl derivatives reduce the viability of cancer cells more strongly than their parent compounds

Derivatives of 2MeTBBi, **14a-b**, inhibit the viability of tumour cells even more effectively than the known approved for clinical trials CK2 inhibitor CX-4945.

The 3D-structures of the CK2 $\alpha^{1-335}$ /**8b** complex were obtained under high salt conditions and under low salt conditions.

Graphical abstract:

